# SUPPLEMENTARY FIGURES

**Supplemental information file list**

**Figure S1.** STF-tagged effector translocation over time, replicate reproducibility and comparison of normalization methods.

**Figure S2.** Connectivity within effector-host protein interaction networks across different conditions tested and enrichment of GroEL in the host cytoplasm upon infection.

**Figure S3.** Comparison of protein expression in RAW264.7 and HeLa cells.

**Figure S4.** Effector translocation and immunoprecipitation in pBMDMs.

**Figure S5.** Cholesterol-trafficking is influenced by a complex interplay of *S*Tm effectors.

**Figure S6.** Characterization of the PipB-PDZD8 interaction.

**Figure S7.** Expression of FMNL1, FMNL2 and FMNL3 in all cell types used for this study.

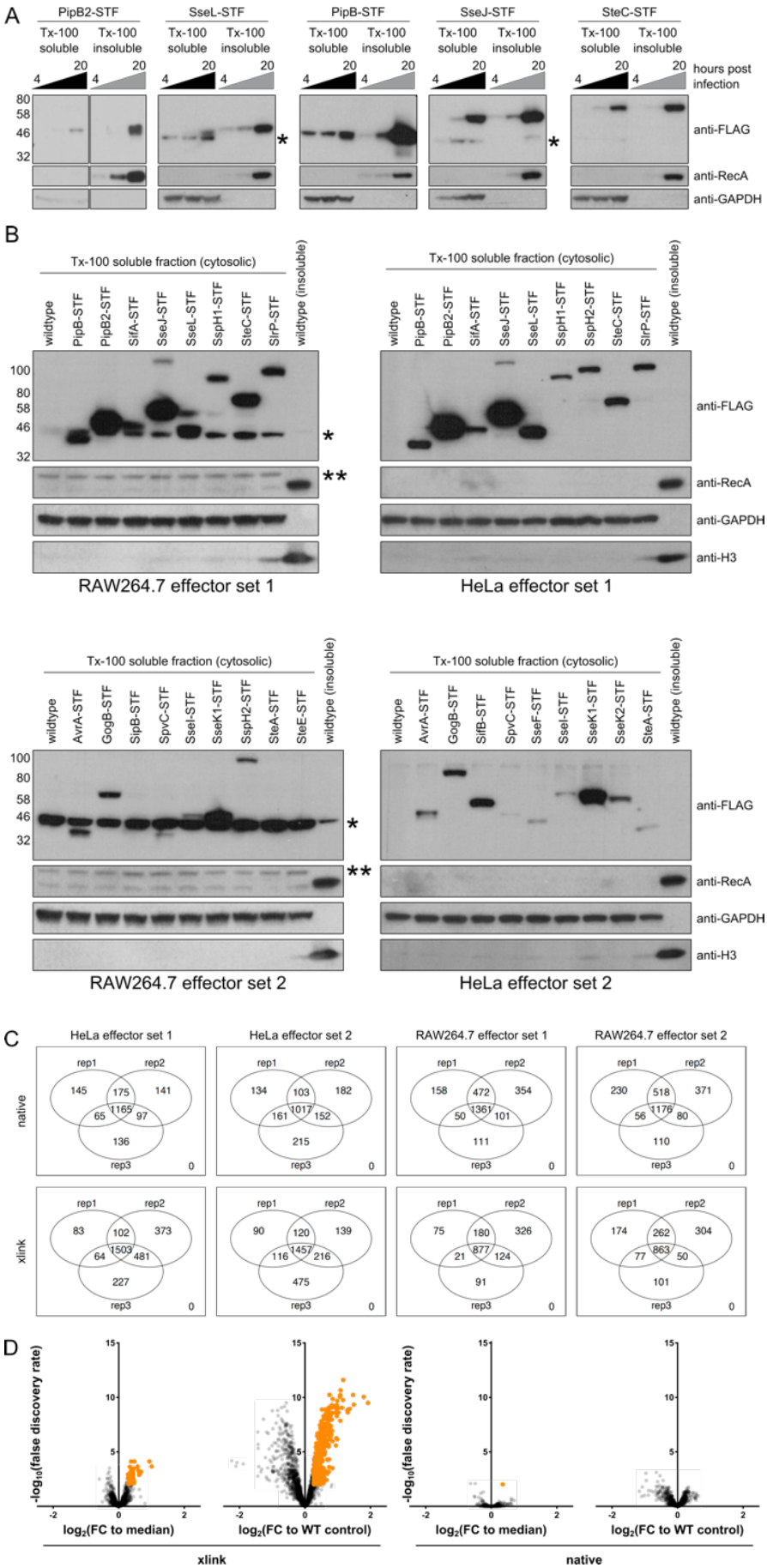
A
PipB2-STF
SseL-STF
PipB-STF
SseJ-STF
SteC-STF
Tx-100 soluble
Tx-100 insoluble
4
20
hours post infection
80
58
46
32
anti-FLAG
anti-RecA
anti-GAPDH
B
Tx-100 soluble fraction (cytosolic)
wildtype
PipB-STF
PipB2-STF
SifA-STF
SseJ-STF
SseL-STF
SspH1-STF
SteC-STF
SlrP-STF
wildtype (insoluble)
100
80
58
46
32
anti-FLAG
anti-RecA
anti-GAPDH
anti-H3
RAW264.7 effector set 1
HeLa effector set 1
AvrA-STF
GogB-STF
SipB-STF
SpvC-STF
SseI-STF
SseK1-STF
SspH2-STF
SteA-STF
SteE-STF
SifB-STF
SseF-STF
SseK2-STF
RAW264.7 effector set 2
HeLa effector set 2
C
HeLa effector set 1
HeLa effector set 2
RAW264.7 effector set 1
RAW264.7 effector set 2
native
xlink
rep1
rep2
rep3
145
175
141
1165
65
97
136
0
134
103
182
1017
161
152
215
158
472
354
1361
50
101
111
230
518
371
1176
56
80
110
83
102
373
1503
64
481
227
90
120
139
1457
116
216
475
75
180
326
877
21
124
91
174
262
304
863
77
50
101
D
-log10(false discovery rate)
log2(FC to median)
log2(FC to WT control)
xlink
native

**Figure S1. STF-tagged effector translocation over time, replicate reproducibility and comparison of normalization methods.**

(A) Time-dependent effector expression and translocation of PipB2, SseL, PipB, SseJ and SteC probed by Western Blot. RAW264.7 were infected with *S*Tm expressing STF-tagged effectors (MOI = 100). 4 hpi, 8 hpi and 20 hpi, cells were lysed in 0.1 % Triton-X100 and the soluble (cytosolic) and insoluble (nuclei, *S*Tm) fractions were separated by centrifugation. Anti-RecA (intact bacteria) and anti-GAPDH (host cytosol) were used as loading controls. Asterisk denotes an unspecific band occurring in RAW264.7 cell lysates that cross-reacts with the M2 FLAG antibody. Time-dependent expression and translocation was assessed in one experiment.

(B) Tagged-effector levels in the host cytoplasm (RAW264.7 and HeLa) at 20 hpi (MOI 100). Samples were prepared as described for panel A. All tagged effectors that were used in AP-QMS are shown in their TMT-multiplexes in the two cell lines, loading controls as in panel A, with anti-H3 for nuclei to assess subcellular fractionation efficiency. Single asterisks as in panel A, double asterisks denote an unspecific band occurring in the cytosolic fraction when probing with RecA-antibody. An additional putative effector not described in this work was measured together with RAW264.7, bringing the total number of effectors to 9.

(C) Venn diagrams summarizing the number of proteins identified in the different replicates of all TMT10 runs. Effector set 1 and 2 refers to the two 10-plexes (WT + 9 effectors) in which the 20 effectors (18 in each of the two cell lines, as depicted in Figure S1B) were split. Only proteins with at least two unique peptides and at least 2 replicates were used for further analysis.

(D) Volcano plots showing fold enrichment for targets identified in RAW264.7 cells after cross-linked (left panels) or native (right panels) pulldown of SteE-STF at 20 hpi (as an example). Fold changes ($Log_2$) for each protein were calculated either with respect to the median abundance across the TMT run (first and third panel) or with respect to the untagged control (second and fourth panel). Hits (fdr < 0.01, FC > 1.2) are colored in orange, all other proteins in grey.

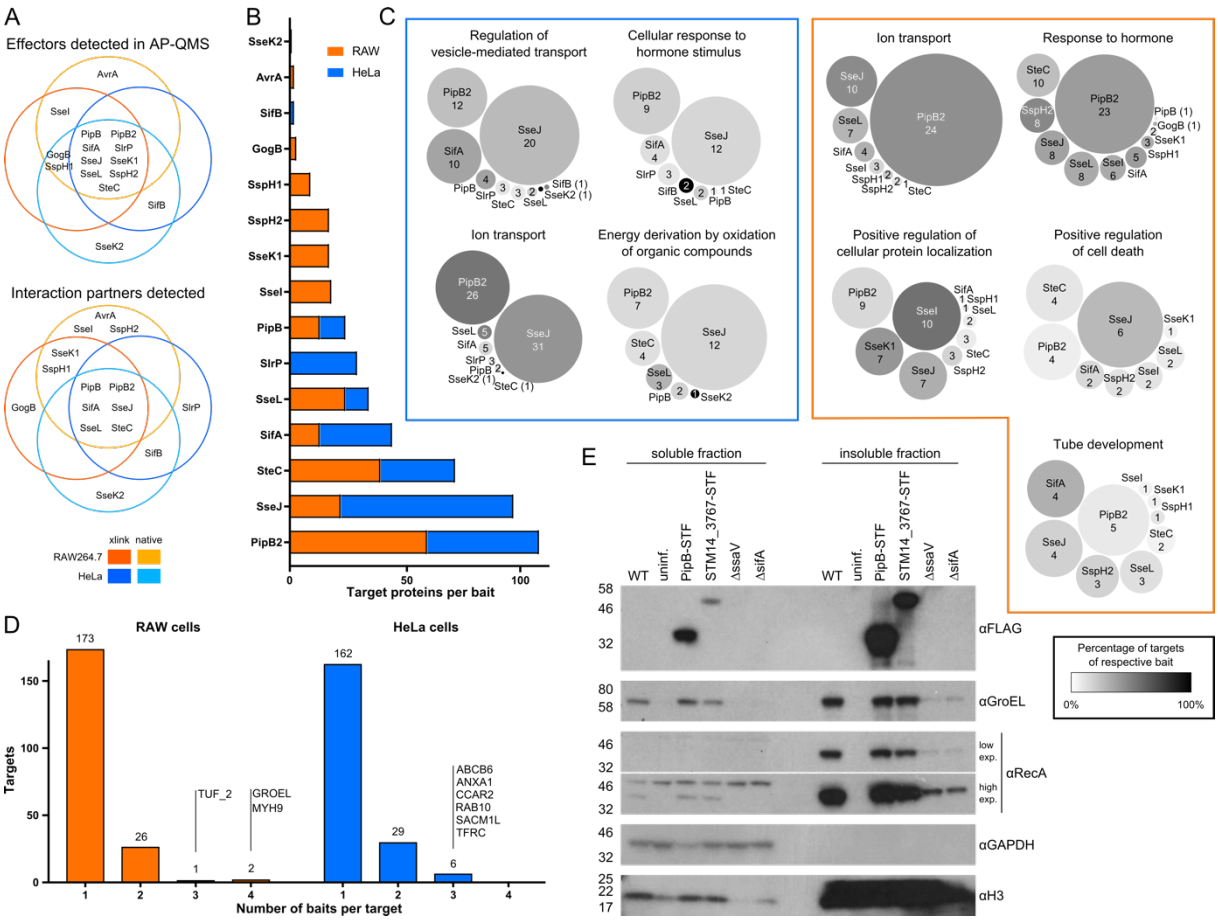


**Figure S2. Connectivity within effector-host protein interaction networks across different conditions tested and enrichment of GroEL in the host cytoplasm upon infection**.

(A) Venn diagrams summarizing which STF-tagged *S*Tm effectors were recovered in the different conditions (upper panel), and for which effectors at least one significantly enriched target protein was identified (lower panel).

(B) Number of target proteins interacting with each effector in RAW264.7 (orange) and HeLa (blue) cells, ordered by total number of protein targets.

(C) Effector-specific GO enrichments. Bubble size corresponds to the percentage of targets associated with a given GO-term interacting with the respective effector (number of eukaryotic protein targets is indicated). Shade of the bubble corresponds to the percentage of target proteins associated with any given GO-term with respect to the total number of proteins interacting with the respective effector (color as indicated in the key). RAW264.7 (orange) and HeLa cells (blue).

(D) Histogram of the number of *S*Tm effector proteins (baits) interacting with each target protein in RAW264.7 (left side, orange) and HeLa cells (right side, blue). Names are indicated for targets with more than 3 PPIs with effectors.

(E) RAW264.7 macrophages were infected with wildtype *S*Tm, several tagged stains and Δ*sifA* and Δ*ssaV* mutants (MOI 100). Experiment was performed as in Figure S1B. In addition to the presence of the effector protein, PipB, in the soluble fraction, we also saw the bacterial proteins GroEL and STM14_3767, a bacterial itaconate CoA-transferase which interacted with PipB in the host cytoplasm, yet not the bacterial loading control RecA. Molecular mass markers are indicated on the left.

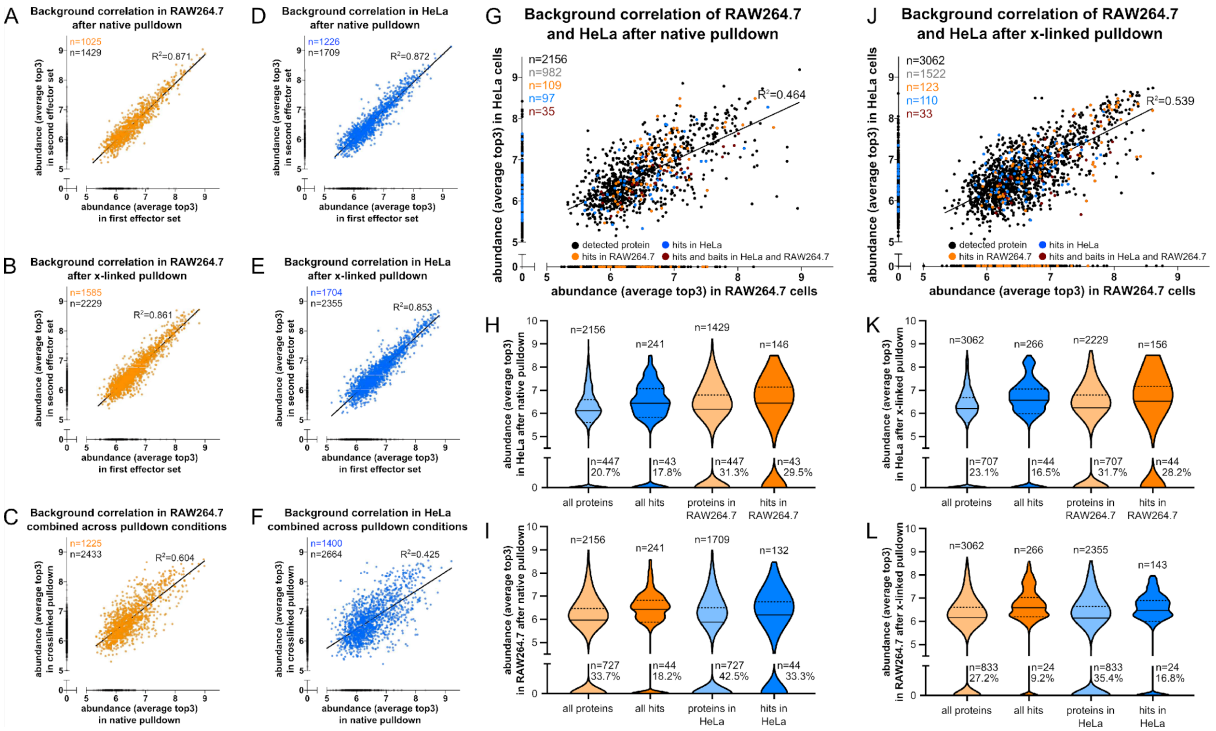


**Figure S3. Comparison of protein expression in RAW264.7 and HeLa cells.**

Orthologs were found based on protein name and using the OMA-browser (Altenhoff et al., 2018) if no ortholog was found. If the protein was not detected in the other cell line, abundance was set to 0 – more detailed information is provided in Experimental Procedures. Correlations of protein abundances in various runs, as indicated in the title of each respective scatter plot.

(A-C) Orange (RAW264.7) and (D-F) blue (HeLa) plots from top to bottom: (A, D) batch comparison in native pulldown; (B, E) batch comparison in pulldown after cross-linking; (C, F) average of native pulldowns vs. average of crosslinked pulldowns.

(G) Native pulldown in RAW264.7 vs. HeLa cells. Hits are indicated: hits in both cell lines in red, hits in HeLa cells only in blue, hits in RAW264.7 cells only in orange.

(H, I) Violin plots summarizing the protein abundance in HeLa epithelial cells (top) and RAW264.7 macrophages (bottom) after native pulldown, i.e. quantification of the x- and y-axis, as well as blue and orange dots of the summarizing scatterplot (panel G). Data presented as in 4C.

(J) Cross-linked pulldown in RAW264.7 *vs* HeLa, hits are annotated as in panel G.

(K, L) Violin plots summarizing panel J, quantification and display as in panels H and I, respectively.

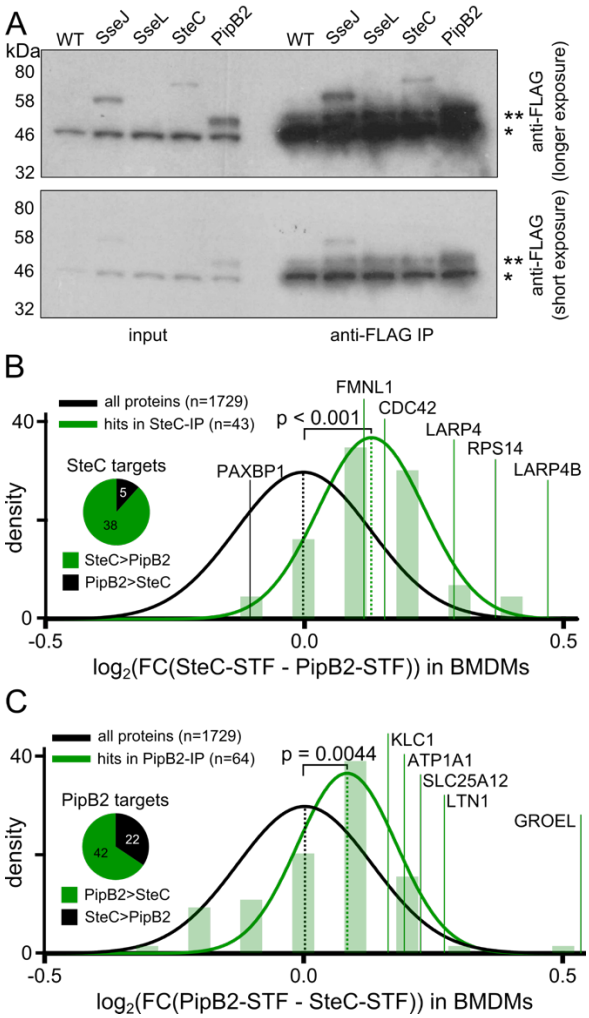


**Figure S4. Effector translocation and immunoprecipitation in pBMDMs.**

(A) Primary murine bone-marrow derived macrophages (pBMDMs) were infected with *S*Tm expressing SseJ-STF, SseL-STF, SteC-STF or PipB2-STF (MOI = 100) and cytosolic fractions were harvested at 20 hpi. Soluble fractions as well as eluates after immunoprecipitation with anti-FLAG(M2) beads were assessed by Western blot using the anti-FLAG(M2) antibody. Single asterisk denotes an unidentified pBMDM protein that cross-reacts with the FLAG antibody, double asterisk denotes a non-specific band in FLAG-pulldown fractions.

(B, C) Density distributions of all proteins (black) and hits for SteC (panel B) and PipB2 (panel C) (green, histograms with bin size 0.1) after AP-QMS in pBMDMs as in A. Nine million cells were infected in triplicate with wildtype *S*Tm, and *S*Tm strains expressing SteC-STF or PipB2-STF. Elution fractions were then measured in a single TMT-10-plex run. Density distributions for all proteins (black) or targets for the respective effector identified in the initial PPI screen in RAW264.7 cells in Figure 2A (green) by effector-effector comparison. Representative hits from RAW264.7 cells are annotated with a line and the dotted line indicates the density median. Two-tailed T-test with Welch correction was performed to assess whether the distributions of hits are significantly different from the distribution of all proteins detected. Pie charts depict the fraction and absolute number of hits identified in the screen that were also more strongly enriched in pBMDMs (green), as well as those that were not (black). Results from LIMMA analysis are located in the corresponding Mendeley Data.

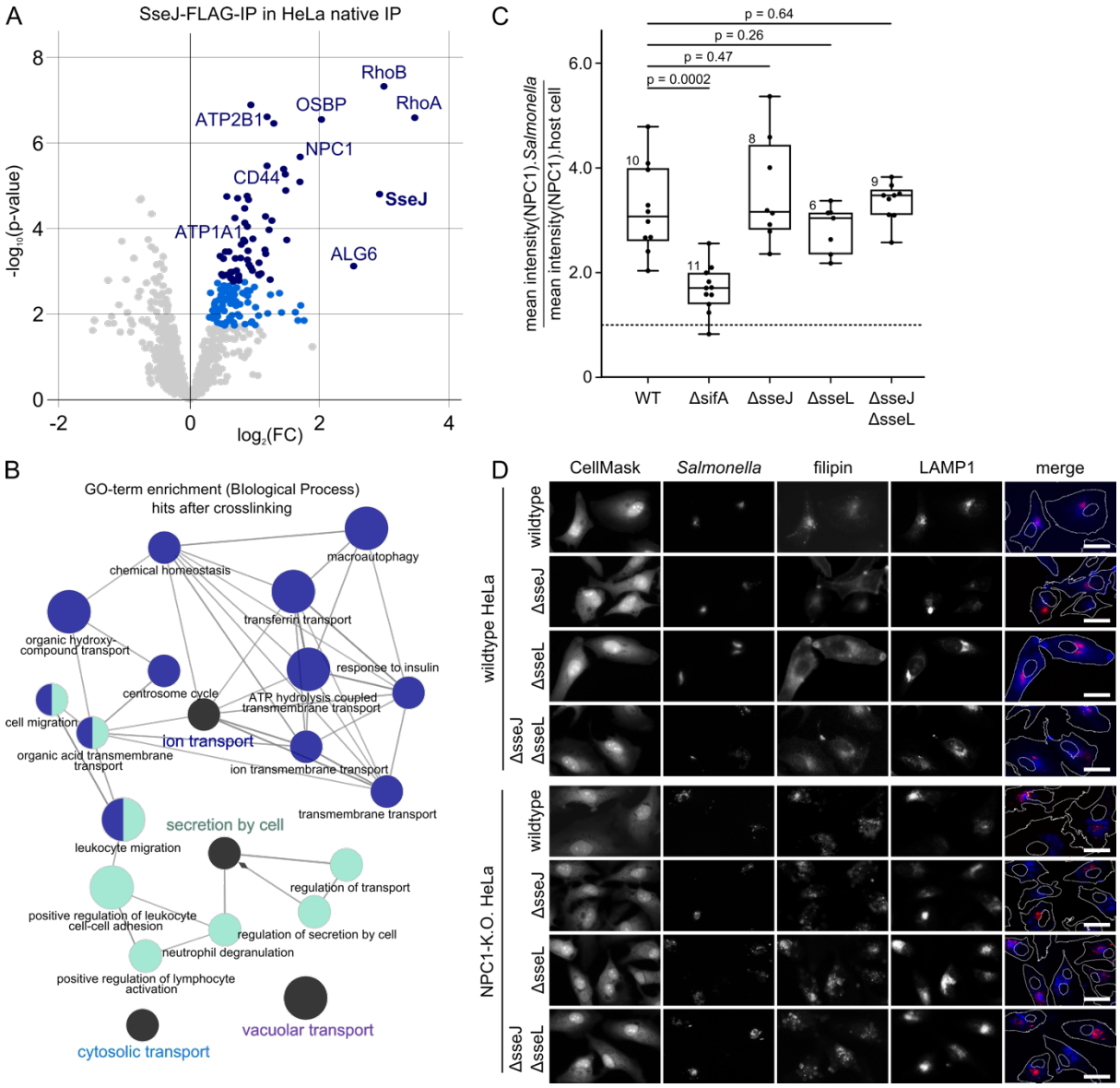


**Figure S5. Cholesterol-trafficking is influenced by a complex interplay of *STm* effectors.**

(A) Volcano plot showing enrichments after native IP of STF-tagged SseJ in HeLa cells at 20 hpi compared to untagged *STm* control (see Figure 5A for pulldown after crosslinking). Three replicates for SseJ-STF and untagged control were measured in a single TMT run. Hit coloring as in 5A.

(B) GO-term network of enriched Biological Processes in the separate SseJ-STF AP-MS (Figure 5A, after crosslinking). GO-terms were required to contain at least 3 genes annotated as hits and a cutoff of $p < 0.05$ after Benjamini-Hochberg correction was applied. Individual GO-terms are shown as bubbles with black labels and clusters after GO-term fusion are shown in the same color as the bubble. Leading GO-term (chosen by number of genes) are indicated in dark grey.

(C) Quantification of colocalization between *STm* and NPC1 in 44 FOVs (wide-field microscopy) obtained after infection and staining as described in Figure 5B. The average NPC1-intensity associated with each *STm* microcolony was divided by the total NPC1-intensity across the entire cell area. Each data point represents one FOV. Boxplot display and statistical tests as in Figure 5C.

(D) Representative microscopy images (20x magnification) of HeLa cells (wildtype and NPC1-knockout) infected with wild type, Δ*sseJ*, Δ*sseL* and Δ*sseJ*/Δ*sseL* *S*Tm expressing mCherry (pFCcGi) at 12 hpi (MOI = 100). Individual channels (HCS CellMask for nuclei, *S*Tm, filipin (detects unesterified cholesterol) and LAMP1) are shown in greyscale and the overlay shows a merge of mCherry-*S*Tm (red) and filipin (blue) signals, with the outlines of the cell periphery and the nuclei drawn in white. Scale bars: 30 μm.

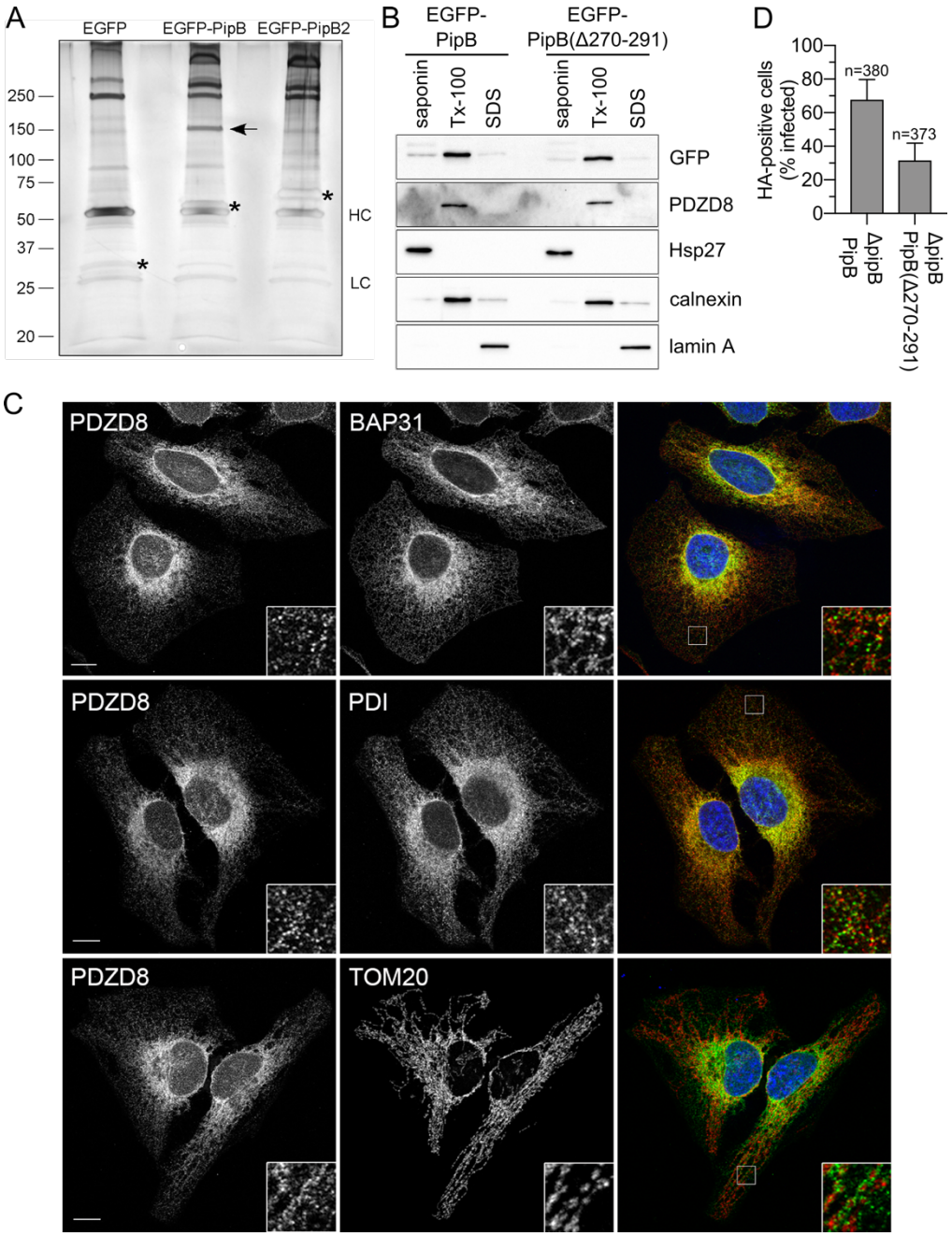


**Figure S6. Characterization of the PipB-PDZD8 interaction.**

(A) Transfected PipB, but not PipB2, interacts with PDZD8. Silver stain of proteins that have been co-immunoprecipitated from HeLa cells expressing either EGFP, EGFP-PipB or EGFP-PipB2. Protein band indicated by arrow in EGFP-PipB lane was analyzed by LC-MS/MS and identified as PDZD8. Asterisks denote EGFP and EGFP-fusion proteins that were immunoprecipitated in each condition. HC, heavy chain; LC, light chain.

(B) PipB and PDZD8 co-fractionate to host cell membranes. HeLa cells were transfected with EGFP-PipB or EGFP-PipB(Δ270-291) and subjected to sequential detergent fractionation as previously described (Lau *et al*., 2019). Saponin-soluble, Tx-100-soluble and SDS-soluble fractions were analyzed by immunoblot with antibodies recognizing GFP, PDZD8, Hsp27 (cytosolic), calnexin (membranes) and lamin A (nuclear).

(C) Localization of endogenous PDZD8 in uninfected cells. HeLa cells were co-stained for BAP31 (integral ER membrane protein), PDI (ER luminal protein) or TOM20 (mitochondrial

transmembrane protein). Merge shows PDZD8 in green and the indicated protein in red, scale bar: 10 µm. Insets show enlargements of indicated areas.

(D) Quantification of PipB translocation by *S*Tm. HeLa cells were infected with *S*Tm$^{SL1344}$ Δ*pipB* (constitutive chromosomal *mCherry* expression) complemented *in trans* with either PipB-2HA or PipB(Δ270-291)-2HA for 12 hpi. Translocated PipB-2HA and PipB (Δ270-291)-2HA was detected by immunostaining with anti-HA antibodies. Four independent experiments were performed and ~100 infected cells were analyzed by fluorescence microscopy per condition. The bars denote the percentage of infected cells where translocated PipB-2HA or PipB (Δ270-291)-2HA was evident. This dataset corresponds to the one analyzed as part of Figure 6G.

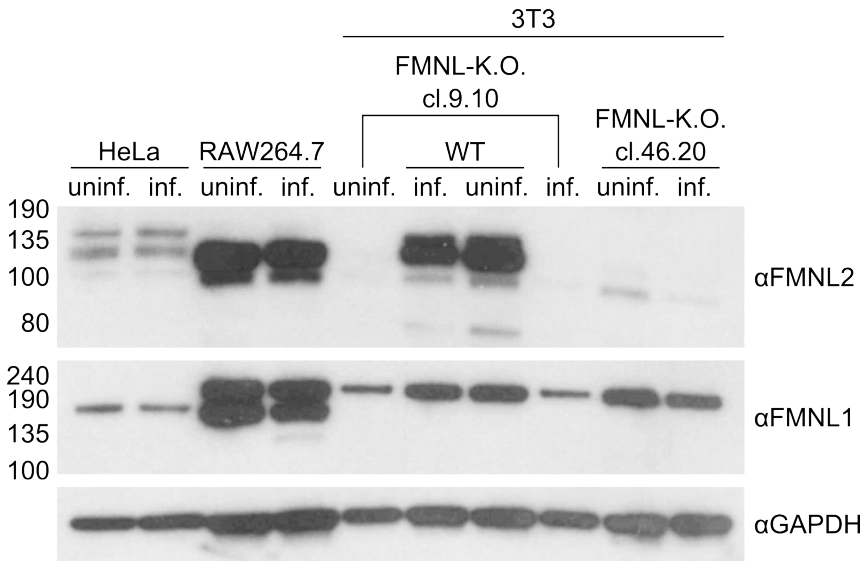


**Figure S7. Expression of FMNL1, FMNL2 and FMNL3 in all cell types used for this study.** Western Blot (performed in a single replicate) showing the presence of FMNLs in the various cell lines used. Protein detection with αFMNL1, αFMNL2 (which also cross-reacts with FMNL3, (Kage et al., 2017a) and αGAPDH antibodies was performed as described in the Experimental Procedures section. Cleared cell lysate (Tx-100-soluble fraction) was loaded in all cases. STm infected samples (inf.) are at 8 hpi (MOI = 100).